

Exploring New Physics in the Electroweak Gauge Sector: Spin Observables and Machine Learning at Future Electron-Positron Colliders.

[Phys.Rev.D 107 \(2023\) 7, 073004](#), [Eur.Phys.J.C 83 \(2023\) 12, 1119](#)

AS&WoMSA, NISER, Bhubaneswar

Amir Subba

Supervisor: Dr. Ritesh Singh

IISER, Kolkata

January 2024

Density Matrices

A quantum state can be represented via density matrices, for e.g;

- spin- $\frac{1}{2}$: $\rho = \frac{1}{2} (\mathbb{I} + P_i \cdot \sigma_i)$
- spin-1 : $\rho = \frac{1}{3} \left[\mathbb{I} + \frac{3}{2} \vec{P} \cdot \vec{S} + \sqrt{\frac{3}{2}} T_{ij} (S_i S_j + S_j S_i) \right]$
- spin- $\frac{3}{2}$: $\rho = \frac{1}{4} \left[\mathbb{I} + 4a_i \Sigma_i + \frac{4}{3} b_{ij} \Sigma_{ij} + \frac{4}{3} c_{ijk} \Sigma_{ijk} \right]$ [hep-ph/1767438](https://arxiv.org/abs/hep-ph/1767438)

The parameters P , T , a , b , c are the vector and tensorial polarizations. Can be obtained from the production part as, $\rho(\lambda, \lambda') \propto \mathcal{M}(\lambda)\mathcal{M}(\lambda')$, and also from the angular distribution of the final decayed particles.

Spin-1: angular distribution function

At the rest frame of the spin-1 mother particle, the angular distribution of the spin-1 particle is [[hep-ph/816419](#)],

$$\begin{aligned} \frac{1}{\sigma} \frac{d\sigma}{d\Omega} = & \frac{3}{8\pi} \left[\left(\frac{2}{3} - (1 - 3\delta) \frac{T_{zz}}{\sqrt{6}} \right) + \alpha P_z \cos \theta + \sqrt{\frac{3}{2}} (1 - 3\delta) T_{zz} \cos^2 \theta \right. \\ & + \left(\alpha P_x + 2\sqrt{\frac{2}{3}} (1 - 3\delta) T_{xz} \cos \theta \right) \sin \theta \cos \theta \\ & + \left(\alpha P_x + 2\sqrt{\frac{2}{3}} (1 - 3\delta) T_{yz} \cos \theta \right) \sin \theta \sin \phi \\ & \left. + (1 - 3\delta) \sin^2 \theta \left(\left(\frac{T_{xx} - T_{yy}}{\sqrt{6}} \right) \cos(2\phi) + \sqrt{\frac{2}{3}} T_{xy} \sin(2\phi) \right) \right] \end{aligned}$$

The parameters of density matrix are obtained by partially integrating such multi dimensional functions.

Case of two spin-1 boson production

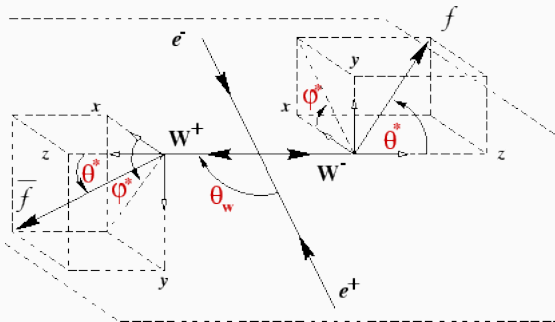


Figure 1: Production and decay of W boson pair, the decay angles are represented at the rest frame of W bosons.

$$\frac{1}{\sigma} \frac{d^2\sigma}{d\Omega^f d\Omega^{\bar{f}}} = \left(\frac{3}{4\pi}\right)^2 \sum_{\lambda_{W-}, \lambda'_{W-}, \lambda_{W+}, \lambda'_{W+}} \rho_{W-W+}(\lambda_{W-}, \lambda'_{W-}, \lambda_{W+}, \lambda'_{W+})$$

$$\times \Gamma_{W-}(\lambda_{W-}, \lambda'_{W-}) \times \Gamma_{W+}(\lambda_{W+}, \lambda'_{W+})$$

The joint density matrix is given as,

$$\begin{aligned}
 \rho_{W^-W^+} = & \frac{1}{9} \left[\mathbb{I}_{9 \times 9} + \frac{3}{2} \vec{P}^{W^-} \cdot \vec{S} \otimes \mathbb{I}_{3 \times 3} + \frac{3}{2} \mathbb{I}_{3 \times 3} \otimes \vec{P}^{W^+} \cdot \vec{S} \right. \\
 & + \sqrt{\frac{3}{2}} T_{ij}^{W^-} (S_i S_j + S_j S_i) \otimes \mathbb{I}_{3 \times 3} + \sqrt{\frac{3}{2}} \mathbb{I}_{3 \times 3} T_{ij}^{W^+} (S_i S_j + S_j S_i) \\
 & + \frac{9}{4} pp_{ij}^{W^-W^+} S_i \otimes S_j + \frac{3}{2} \sqrt{\frac{3}{2}} p T_{ijk}^{W^-W^+} S_i \otimes (S_j S_k + S_k S_j) \\
 & + \frac{3}{2} \sqrt{\frac{3}{2}} T p_{ijk}^{W^-W^+} (S_i S_j + S_j S_i) \otimes S_k \\
 & \left. + \frac{3}{2} TT_{ijkl}^{W^-W^+} (S_i S_j + S_j S_i) \otimes (S_k S_l + S_l S_k) \right].
 \end{aligned}$$

Apart from the usual polarizations, there are parameters such as $pp^{W^-W^+}$, $pT/Tp^{W^-W^+}$, and $TT^{W^-W^+}$ which are various correlations. In total, we will have 80 independent spin observables.

How to obtain those parameters?

- Analytically, $\rho \propto \mathcal{M}(\lambda_{W-}, \lambda_{W+})\mathcal{M}(\lambda'_{W-}, \lambda'_{W+})$
- From the asymmetries of angular distribution of decayed fermions, for e.g. [[hep-ph/1028972](#)],
- $$P_x^W = \frac{2}{\alpha} \left(\int_{\theta=0}^{\pi} \int_{\phi=-\pi/2}^{\pi/2} - \int_{\theta=0}^{\pi} \int_{\phi=\pi/2}^{3\pi/2} \right) d\Omega \left(\frac{1}{\sigma} \frac{d\sigma}{d\Omega} \right),$$
$$\equiv \frac{4}{3\pi} \frac{\sigma(\sin\theta \cos\phi > 0) - \sigma(\sin\theta \cos\phi < 0)}{\sigma(\sin\theta \cos\phi > 0) + \sigma(\sin\theta \cos\phi < 0)}$$
- $$T_{zz}^W = \frac{\pi}{2} \sqrt{\frac{3}{2}} \frac{1}{1-3\delta} \frac{\sigma(\sin(3\theta) > 0) - \sigma(\sin(3\theta) < 0)}{\sigma(\sin(3\theta) > 0) + \sigma(\sin(3\theta) < 0)}$$

Here α , and δ are the parameters that depend on the chiral couplings and the mass of the final fermions. α also decides the purity of the polarization information of mother particle.

CP structure of asymmetries

σ	A_x	A_y	A_z	A_{xy}	A_{xz}	A_{yz}	$A_{x^2-y^2}$	A_{zz}
A_x	E	O	E	O	E	O	E	E
A_y	O	E	O	E	O	E	O	O
A_z	E	O	E	O	E	O	E	E
A_{xy}	O	E	O	E	O	E	O	O
A_{xz}	E	O	E	O	E	O	E	E
A_{yz}	O	E	O	E	O	E	O	O
$A_{x^2-y^2}$	E	O	E	O	E	O	E	E
A_{zz}	E	O	E	O	E	O	E	E

Figure 2: CP structure of polarization and correlation asymmetries; letter E and O represents CP-even and odd, and the color red suggest flavor tagging and blue are immune to flavor identity.

Light Flavor Tagging with Machine Learning

- Hardest two jets are chosen.
- $R_{qj} = \sqrt{(\Delta\eta_{qj})^2 + (\Delta\phi_{qj})^2}$: Truth labeling
- Features are extracted from the constituents of two jets.
- Displaced tracks, leptons, Kaons, and Pions are some of the significant features.
- Artificial and convolutional neural networks, boosted decision trees are developed.
- All the networks are almost equivalent in classifying; BDT is pretty fast.
- Accuracy of around 80% is achieved (**need to improve!**)

What can we do with all these?

The spin of a particle determines the Lorentz structure of its couplings with the other SM fermions and bosons. This, in a way, fixes its dominant production and decay mechanisms. Assuming new physics to be heavy, $\Lambda > \sqrt{\hat{s}}_{\text{LHC}}$, a model independent approach is taken with the heavy degree of freedom integrated out. The effect of new physics is encoded in the Wilson coefficient at the electroweak scale. One important platform provided by $W^- W^+ Z/\gamma$ coupling, which in presence of relevant dimension-6 operators is [[hep-ph/353285](https://arxiv.org/abs/hep-ph/353285)],

$$\begin{aligned}\mathcal{L}_{(6)} = & \mathcal{L}_{(4)} + \frac{c_{WWW}}{\Lambda^2} \text{Tr}[W_{\nu\rho} W^{\mu\nu} W_{\rho}^{\mu}] + \frac{c_W}{\Lambda^2} (D_{\mu}\Phi)^{\dagger} W^{\mu\nu} (D_{\nu}\Phi) \\ & + \frac{c_B}{\Lambda^2} (D_{\mu}\Phi)^{\dagger} B^{\mu\nu} (D_{\nu}\Phi) + \frac{c_{\widetilde{WWW}}}{\Lambda^2} \text{Tr}[\widetilde{W}_{\mu\nu} W^{\nu\rho} W_{\rho}^{\mu}] \\ & + \frac{c_{\widetilde{W}}}{\Lambda^2} (D_{\mu}\Phi)^{\dagger} \widetilde{W}^{\mu\nu} (D_{\nu}\Phi)\end{aligned}$$

Analysis at e^-e^+ Collider

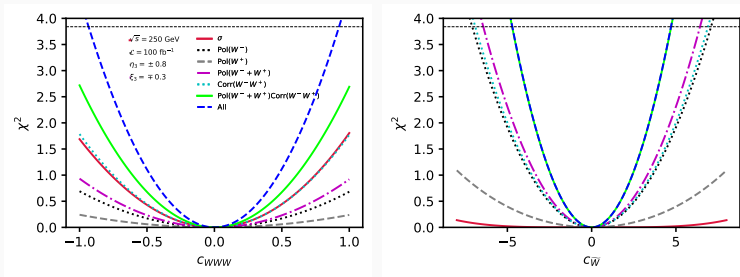


Figure 3: One parameter limits on the anomalous couplings as a function of various set of observables. The combination of spin related observables provides a tighter constraint.

Why better Tagger?

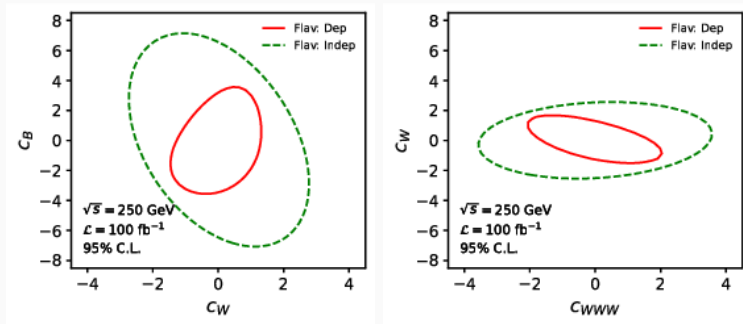


Figure 4: Two parameter limits on the anomalous couplings as a function of various set of flavor dependent and independent observables. The cross section is not included for this presentation.

Polarized beams

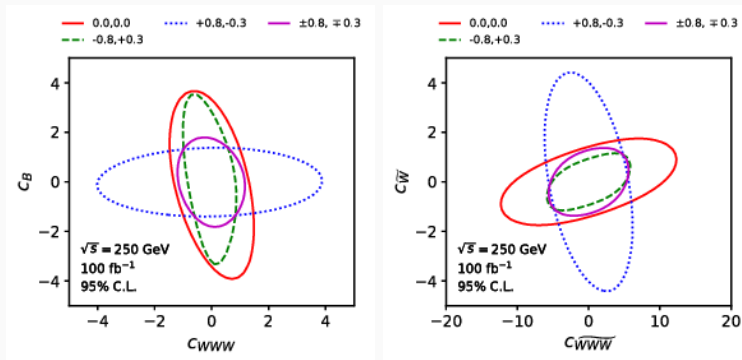


Figure 5: Two parameter limits on the anomalous couplings as a function of different set of initial beam polarization. The value of polarization is set to initial target of International Linear Collider. The use of flip polarization provides a directional cut in the contour leading to tighter bounds.

Marginalized Bounds

Perform a Markov-Chain-Monte-Carlo analysis with all set of observables, and beam polarization.

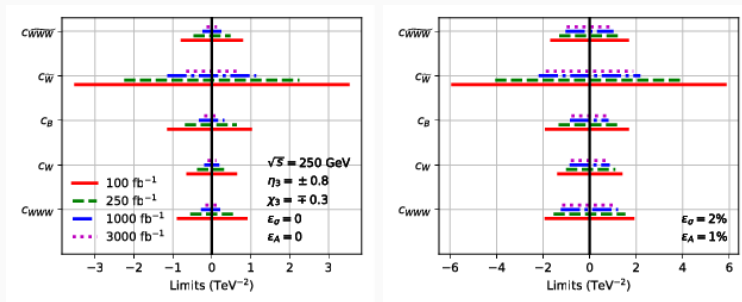


Figure 6: Marginalized limits on the anomalous couplings as a function of different set of integrated luminosity and systematic errors. Immediate observation is that even with large datasets if systematic errors are not reduced, there is not much gain on the bounds.

A walk further into quantum structure through entanglement

Entanglement is an extreme case of correlations without classical analogue. Quantum state is describe by the density matrix, e.g, for a case of two qubit, the joint density matrix is given by,

$$\rho = \frac{1}{4} (\mathbb{I}_{4 \times 4} + \mathbb{I}_{2 \times 2} \otimes \vec{p}^+ \cdot \sigma + \vec{p}^- \cdot \sigma \otimes \mathbb{I}_{2 \times 2} + c_{ij} \sigma_i \otimes \sigma_j)$$

The violation of Bell's inequalities can be performed with the measurable quantity called concurrence,

$\rho = \max(0, \lambda_1 - \lambda_2 - \lambda_3 - \lambda_4)$ where λ 's are the eigenvalues of matrix,

$$C[\rho] = \sqrt{\sqrt{\rho} (\sigma_2 \otimes \sigma_2) \rho^* (\sigma_2 \otimes \sigma_2) \sqrt{\rho}}$$

Also have varied form, like the one ATLAS calculated,

$D = -3\langle \cos \psi \rangle$ for the $t\bar{t}$ case [[hep-ph/2721895](https://arxiv.org/abs/hep-ph/2721895)].

Table 1: Logarithmic negativity for different di-boson production processes at e^-e^+ Collider at $\sqrt{s} = 1$ TeV and pp Collider at $\sqrt{s} = 13$ TeV. The measure of entanglement is listed for different region of production angle and invariant mass of di-boson.

Coll	Bins	$\text{Log}_3(\text{Tr} [\tilde{\rho}^\dagger \tilde{\rho}])$		Coll	Bins	$\text{Log}_3(\text{Tr} [\tilde{\rho}^\dagger \tilde{\rho}])$		
		$W^- W^+$	ZZ			$W^- W^+$	ZZ	ZW
e^-e^+	Unbinned	0.348	0.271	pp	Unbinned	0.475	0.474	0.198
	$-1.0 \leq \cos \theta < -0.75$	1.961	0.378		$0.0 \leq m_{VV} \leq 200.0$	0.637	0.525	0.286
	$-0.75 \leq \cos \theta < -0.5$	1.373	0.699		$200.0 < m_{VV} \leq 300.0$	0.563	0.589	0.2248
	$-0.5 \leq \cos \theta < -0.25$	1.278	0.839		$300.0 < m_{VV} \leq 400.0$	0.397	0.594	0.283
	$-0.25 \leq \cos \theta < 0.0$	1.376	0.984		$400.0 < m_{VV} \leq 500.0$	0.368	0.361	0.551
	$0.0 \leq \cos \theta < 0.25$	1.260	1.060		$500.0 < m_{VV} \leq 600.0$	0.675	0.330	0.360
	$0.25 \leq \cos \theta < 0.5$	0.909	0.945		$600.0 < m_{VV} \leq 700.0$	0.811	0.968	0.594
	$0.5 \leq \cos \theta < 0.75$	0.819	0.537		$700.0 < m_{VV} \leq 800.0$	1.373	1.147	1.117
$0.75 \leq \cos \theta \leq 1.0$	0.359	0.335	$800.0 < m_{VV}$	0.572	1.049	0.442		

Tripartite entanglement with $t\bar{t}Z$ process

		$C_{t\bar{t}}$	C_{tZ}	$C_{\bar{t}Z}$	$C_{t\bar{t}Z}$	$C_{\bar{t}tZ}$	$C_{Z t\bar{t}}$	$\text{GME}_{t\bar{t}Z}$
	Un-bin	0	0	0	0	0	0	0
SM	$\sqrt{\hat{s}} < 0.5$ TeV	0	0	0	0.00341	0.0028	0.00697	0.00354
	$0.5 < \sqrt{\hat{s}} < 1$ TeV	0	0	0	0	0	0	0
	$1 < \sqrt{\hat{s}} < 1.5$ TeV	0	0	0	0	0	0	0
	$\sqrt{\hat{s}} > 1.5$ TeV	0	0	0	0.00795	0.00739	0.00829	0.00786
	$\sqrt{\hat{s}} < 1.5$ TeV	0	0	0	0	0	0	0
	Un-bin	0	0	0	0.0176	0.0184	0.0244	0.0197
dim-8	$\sqrt{\hat{s}} < 0.5$ TeV	Not enough events						
	$0.5 < \sqrt{\hat{s}} < 1$ TeV	0.666	0.0125	0	0.615	0.615	0.213	0.399
	$1 < \sqrt{\hat{s}} < 1.5$ TeV	0.694	0	0	0.563	0.563	0.11	0.28
	$\sqrt{\hat{s}} > 1.5$ TeV	0.712	0	0.00299	0.545	0.545	0.0349	0.158
	$\sqrt{\hat{s}} < 1.5$ TeV	0.688	0	0	0.537	0.537	0.084	0.24

Conclusions

- Polarizations and spin correlations provides a set of sensitive observables to new physics.
- Higher order corrections becomes important ([This school!](#))
- Measure of entanglement as a probe to beyond SM parameters.

Thank you for your Time!!

- $\mathcal{E}_N(\rho) = \text{Log}_3(\|\tilde{\rho}\|_1)$, where $\|\cdot\|_1$ represents the trace norm, and $\tilde{\rho}$ is the state obtained after doing a partial trace of one of the subsystems, $\tilde{\rho}_{ij,kl} = \rho_{il,jk}$.
- $GME_{\bar{t}Z} \equiv \left[\frac{16}{3} Q(Q - \mathcal{C}_{A|(BC)})Q(Q - \mathcal{C}_{B|(AC)})(Q - \mathcal{C}_{C|(AB)}) \right]$
 $Q = \frac{1}{2} (\mathcal{C}_{A|(BC)} + \mathcal{C}_{B|(AC)} + \mathcal{C}_{C|(AB)})$